Leukocyte-inspired biodegradable particles that selectively and avidly adhere to inflamed endothelium *in vitro* and *in vivo*

Harshad S. Sakhalkar*, Milind K. Dalal*, Aliasger K. Salem†, Ramin Ansari‡, Jie Fu§, Mohammad F. Kiani‡, David T. Kurjiaka¶, Justin Hanes§, Kevin M. Shakesheff†, and Douglas J. Goetz*‖

Departments of *Chemical Engineering and ¶Biological Sciences, Ohio University, Athens, OH 45701; †School of Pharmaceutical Sciences, University of Nottingham, Nottingham NG7 2RD, United Kingdom; ‡Department of Biomedical Engineering, University of Tennessee Health Science Center, Memphis, TN 38163; and §Department of Chemical and Biomolecular Engineering, Johns Hopkins University, Baltimore, MD 21218

Edited by Robert Langer, Massachusetts Institute of Technology, Cambridge, MA, and approved October 29, 2003 (received for review March 12, 2003)

We exploited leukocyte–endothelial cell adhesion chemistry to generate biodegradable particles that exhibit highly selective accumulation on inflamed endothelium *in vitro* and *in vivo*. Leukocyte–endothelial cell adhesive particles exhibit up to 15-fold higher adhesion to inflamed endothelium, relative to noninflamed endothelium, under *in vitro* flow conditions similar to that present in blood vessels, a 6-fold higher adhesion to cytokine inflamed endothelium relative to non-cytokine-treated endothelium *in vivo*, and a 10-fold enhancement in adhesion to trauma-induced inflamed endothelium *in vivo* due to the addition of a targeting ligand. The leukocyte–inspired particles have adhesion efficiencies similar to that of leukocytes and were shown to target each of the major inducible endothelial cell adhesion molecules (E-selectin, P-selectin, vascular cell adhesion molecule 1, and intercellular adhesion molecule 1) that are up-regulated at sites of pathological inflammation. The potential for targeted drug delivery to inflamed endothelium has significant implications for the improved treatment of an array of pathologies, including cardiovascular disease, arthritis, inflammatory bowel disease, and cancer.

The expression of endothelial cell adhesion molecules (ECAMs) known to play a role in leukocyte recruitment [i.e., vascular cell adhesion molecule (VCAM)-1, E-selectin, P-selectin, and intercellular adhesion molecule (ICAM)-1] is increased at sites of pathological inflammation. For example, VCAM-1 is present in a localized fashion on aortic endothelium that overlies early foam cell lesions (1) and is increased on endothelium in models of colitis (2). P-selectin and E-selectin are up-regulated in a variety of pathological settings, including ischemia-reperfusion injury (3), arthritis (4), and colitis (5). ICAM-1 expression is increased in ischemia-reperfusion injury (3) and at sites of radiation-induced inflammation (6, 7). Additionally, the expression of these ECAMs may be increased on endothelium within tumors (e.g., ref. 8).

These observations have led to a strong interest in the development of drug delivery strategies that exploit the increased expression of ECAMs to achieve selective delivery to sites of diseased tissue (9–12). Drug carriers made from biodegradable polymers [e.g., poly(lactic acid), PLA] are easily prepared, have a long shelf life, can carry several orders of magnitude more drug than a mAb, and can be designed to have well defined drug-release rates (13–15). Because of these attributes, it is well accepted that biodegradable drug carriers complement and expand the possibilities of targeted drug delivery afforded by other carriers (e.g., liposomes and mAbs) (14).

Recent studies have attempted to develop biodegradable particles that exhibit selective adhesion to ECAM-expressing endothelium. Previously, our group passively adsorbed a mAb to E- and P-selectin onto poly(ε-caprolactone) (PCL) particles and found that the resulting mAb-coated PCL particles exhibited selective adhesion to cells expressing E- and P-selectin (16). However, the adhesion was low ($<0.17\%$ that of leukocytes) and occurred only at shear stresses ≤ 0.3 dynes/cm^2, a level of shear that is not considered physiologically relevant (16). The limited adhesion appeared to be due to a low level of mAb adsorbed to the particles. Another group has conjugated SLe^x (a carbohydrate ligand for selectins) to biodegradable particles and found that the SLe^x particles roll on polystyrene surfaces coated with purified P-selectin (17). However, the adhesion of the particles to endothelial cells *in vitro* and the interaction of the particles with the vasculature *in vivo* were not determined. It should also be noted that neither of the polymers used previously (16, 17) had incorporated stealth chemistry [e.g., poly(ethylene glycol) (PEG)] that would presumably be needed to achieve reasonable circulation times *in vivo* (18, 19). Thus, to date the goal of developing biodegradable particles that avidly and selectively adhere to inflamed endothelium has remained elusive.

In this paper, we describe the development of targeted, PEGylated biodegradable particles that have adhesive properties similar to that of leukocytes. The targeted particles exhibit (*i*) significant (up to 15-fold) selective adhesion to inflamed endothelium, relative to noninflamed endothelium, under physiologically relevant *in vitro* flow conditions, (*ii*) significant (6-fold) selective adhesion for cytokine inflamed endothelium, relative to non-cytokine-treated endothelium, *in vivo*, and (*iii*) significant (up to 10-fold) enhancement in adhesion to trauma-induced inflamed endothelium, *in vivo*, due to the addition of a targeting ligand. We demonstrate that the particles can be made to target all of the major inducible ECAMs (E-selectin, P-selectin, VCAM-1, and ICAM-1) that have been shown to be up-regulated in a host of disease settings (1–7). The design of these particles and this targeting approach in general, is inspired by the leukocyte–endothelial cell biochemistry that mediates the selective recruitment of leukocytes to a site of inflammation. Thus, by bridging the fields of drug delivery and vascular cell–cell adhesion, we have successfully developed PEGylated biodegradable polymeric particles that exhibit selective adhesion to inflamed endothelium at levels similar to that of leukocytes.

Materials and Methods

Materials. PBS and Hanks' balanced salt solution (HBSS) with Ca^{2+} and Mg^{2+} (HBSS+) were from BioWhittaker (Walkersville, MD). BSA was from Sigma and added to PBS to make the blocking buffer (PBS, 1% BSA). FBS was added to HBSS+, 1% BSA to make the assay buffer (HBSS+, 1% BSA, 2% FBS).

This paper was submitted directly (Track II) to the PNAS office.

Abbreviations: LEAP, leukocyte–endothelial cell adhesive particle; ECAM, endothelial cell adhesion molecule; TNF-α, tumor necrosis factor α; HUVEC, human umbilical vein endothelial cells; PEG, poly(ethylene glycol); PLA, poly(lactic acid); FACS, fluorescence-activated cell sorting; VCAM-1, vascular cell adhesion molecule 1; ICAM-1, intercellular adhesion molecule 1.

‖To whom correspondence should be addressed. E-mail: goetzd@ohio.edu.

Neutravidins were from Molecular Probes. Recombinant mouse tumor necrosis factor α (TNF-α) was from Calbiochem. All reagents for culturing and activating human umbilical vein endothelial cells (HUVEC) were as described (20).

Biotin–caproyl–protein A was from Accurate Chemical and Scientific (Westbury, NY). The 19.ek.Fc PSGL-1 construct is a chimera consisting of the first 19 aa of mature PSGL-1 linked to an enterokinase cleavage site, which, in turn, is linked to the Fc region of human IgG1. Fc liberated by enterokinase (ek.Fc) served as a negative control. The 19.ek.Fc, ek.Fc, and murine mAb HPDG2/3 (anti-human P-selectin; IgG1) were provided by Raymond T. Camphausen (Wyeth Research, Cambridge, MA) and have been described (21, 22). Murine mAb KPL-1 (anti-human PSGL-1; IgG1), murine biotinylated mAb 68–5H11 (anti-human E-selectin; IgG1), rat biotinylated mAb 10E9.6 (anti-murine E-selectin; IgG2a), biotinylated rat IgG2a, and biotinylated mouse IgG1 were from Pharmingen. Murine biotinylated mAb 15.2 (anti-human ICAM-1; IgG1) and biotinylated mAb 1.G11B1 (anti-human VCAM-1; IgG1) were from Calbiochem.

HUVEC Culture. HUVEC were purchased from Clonetics (San Diego, CA) and maintained in culture as described (21). HUVEC were activated by 4-h treatment with 0.25 ng/ml IL-1β or 25 ng/ml TNF-α. Note that, in preliminary experiments, we characterized the adhesion molecule profile on unactivated, 4-h IL-1β-, and 4-h TNF-α-activated HUVEC by using ELISA. The adhesion molecule profiles on our HUVEC, described in *Results and Discussion*, are similar to that reported by others (23).

PLA–PEG–Biotin Synthesis. We generated a PLA–PEG–biotin polymer for the present study as described (24, 25). In brief, 1 g of α-amine-ω-hydroxy PEG (Shearwater Polymers, average molecular mass, 3.4 kDa) was stirred with 0.250 g of *N*-hydroxysuccinimide–biotin (Sigma) and 80 μl of triethylamine in 1 ml of dichloromethane and 2 ml of acetonitrile at room temperature under argon overnight. Biotinylated PEG was isolated by dissolving in hot isopropanol and then cooling. The resulting precipitate was collected by vacuum filtration and dried from toluene azeotrope. Second, 2.0 g of D,L-lactide (Purac, Lincolnshire, IL) was polymerized with 0.35 g of ω-hydroxy PEG-biotin by using 0.1 g of stannous 2-ethyl hexanoate (Sigma) as the initiator by reflux in silanized glassware containing 25 ml of anhydrous toluene to yield PLA–PEG–biotin. The final polymeric material was recovered by dissolution in 10 ml of dichloromethane and precipitation in 200 ml of cold ether.

PLA–PEG–Biotin Particle Synthesis. Particles were produced by using a single emulsion technique in which 10 ml of a 25 mg/ml solution of the polymer in dichloromethane was homogenized for 2 min in 250 ml of a 0.1% (wt/vol) aqueous poly(vinyl alcohol) (PVA) solution (PVA 88% hydrolyzed, PolySciences, Warrington, PA). In certain cases, rhodamine was added to the organic phase to produce rhodamine-loaded PLA–PEG particles. The resulting emulsion was stirred for 4 h at room temperature in a chemical fume hood to allow the dichloromethane to evaporate. Particles were collected by centrifugation, washed in distilled water, and then freeze-dried. Particle size analysis was performed with a Coulter Multisizer II (Beckman Coulter). Batches with number average diameters between 1.0 and 2.5 μm were used in this study.

Ligand Conjugation to PLA–PEG–Biotin Particles. PLA–PEG–biotin particles were incubated (7.5×10^7 particles per ml, 37°C for 20 min) in PBS containing 50 μg/ml neutravidin. Neutravidin Texas Red was used when preparing PLA–PEG particles for the *in vitro* adhesion assays, and neutravidin Oregon Green was used when preparing PLA–PEG particles for the 19.ek.Fc *in vivo* assays. All other preparations were done with unconjugated neutravidin. PLA–PEG–biotin particles with incorporated rhodamine were used in the TNF-α *in vivo* experiments. Neutravidin-conjugated PLA–PEG particles were washed and incubated (2×10^7 particles per ml, 24°C, 30 min) in PBS containing a biotinylated mAb (various concentrations), biotinylated mouse or rat IgG (30 μg/ml; 60 μg/ml), or biotinylated protein A (50 μg/ml). With the exception of the protein A PLA–PEG particles, the resulting mAb or IgG-conjugated PLA–PEG particles were washed with blocking buffer and held in blocking buffer at room temperature (<4 h) until used in the fluorescence-activated cell sorting (FACS) or adhesion assays. Washed protein A PLA–PEG particles were incubated (4×10^7 particles per ml, 24°C, 1 h) in blocking buffer containing 17 μg/ml of the 19.ek.Fc or ek.Fc construct. The resulting suspension was stored overnight at 4°C before performing the *in vivo* assays. For the FACS assays, the 19.ek.Fc and ek.Fc particles were washed in blocking buffer and immediately used.

Flow Cytometric Analysis. mAb conjugated PLA–PEG particles were incubated (24°C, 20 min) with a FITC-conjugated goat $F(ab')_2$ polyclonal anti-mouse (Caltag, Burlingame, CA) or anti-rat antibody (Jackson ImmunoResearch), washed and fixed in HBSS+ containing 1% formaldehyde. 19.ek.Fc and ek.Fc PLA–PEG particles were incubated (24°C, 20 min) with mAb KPL-1 or HPDG2/3, washed, incubated (24°C, 20 min) with an FITC polyclonal antibody to mouse IgG, washed and fixed in HBSS+ containing 1% formaldehyde. Fluorescence of PLA–PEG particles was determined by using a FACSort flow cytometer (Beckon Dickinson). To gain insight into the number of mAbs bound to the PLA–PEG particles, Quantum Simply Cellular beads (Bangs, Fishers, IN), which have a known number of binding sites for mouse IgG, were used to calibrate the flow cytometer as per the manufacturer's instructions.

***In Vitro* Adhesion Assay.** A parallel plate flow chamber (Glycotech, Rockville, MD), similar to that described by Smith and colleagues (26), was used in this study. Our particular set up has been described (20). An image intensifier was used to enhance detection of the PLA–PEG particles. A suspension of PLA–PEG particles (6×10^5 in assay buffer) was drawn over the HUVEC at 1.5 dynes/cm^2. After 2.5 min of flow, the number of PLA–PEG particles adherent to the HUVEC was determined for eight different fields of view under fluorescence illumination. These numbers were averaged and normalized to the area of the field of view to give an n of 1. The results of n replicate experiments were averaged to give the data presented.

***In Vivo* Adhesion Assay.** We used intravital microscopy as described (27). Briefly, animals were intubated, catheterized, and placed on a surgical board where the right cremaster muscle was pinned as a flat sheet. In certain cases, the mice were given an intrascrotal injection of TNF-α (500 ng in saline) 2 h before the surgery. Approximately 20 min after surgery, the PLA–PEG particles were injected (femoral artery for the trauma model and jugular vein for the TNF-α model). The number of adherent (either rolling or firmly adherent) PLA–PEG particles was determined by observing postcapillary venules through an intravital microscope by using fluorescent illumination and normalized to the length of the venule, for firm adhesion, and the length of the venule and the time of observation, for rolling adhesion. Data were collected from $n \geq 3$ separate mice for each condition. These values were averaged to obtain the data presented.

Statistical Analysis. Student's t test was used to analyze the difference between two means. Multiple comparisons against a single control were evaluated by using ANOVA and, subse-

quently, a Bonferroni test was used to determine statistical significance. In all instances, comparisons with P values <0.05 were considered statistically significant. All error bars represent standard deviation.

Results and Discussion

PLA–PEG Particles Conjugated with mAbs to Inducible ECAMs Exhibit Significant Selective Adhesion to Inflamed HUVEC Under Physiologically Relevant *in Vitro* Flow Conditions. We sought to determine whether biodegradable particles conjugated with ligands to inducible ECAMs could exhibit selective adhesion to inflamed endothelium *in vitro*. We used HUVEC as our model endothelial cell because HUVEC are of human origin, well characterized, widely used to investigate vascular events *in vitro* (e.g., articles citing ref. 28), and can be treated with cytokines to generate an *in vitro* model of inflamed endothelium (23). The adhesion molecule profile on the HUVEC used in this study, as determined by ELISA (data not shown), is similar to that reported by others (23). Specifically, HUVEC cultured in the absence of activating agents (e.g., IL-1β or TNF-α), have little, if any, surface expression of E-selectin, VCAM-1, or P-selectin, but do express ICAM-1. A 4-h treatment of HUVEC with the proinflammatory cytokines TNF-α or IL-1β induces E-selectin expression and increases ICAM-1 expression. A 4-h treatment of HUVEC with TNF-α induces significant and reproducible VCAM-1 expression. We did not detect P-selectin surface expression on 4-h IL-1β- or TNF-α-treated HUVEC.

Shakesheff and coworkers (24, 25, 29) have recently developed a biodegradable block copolymer consisting of biotinylated PEG and PLA blocks. The phase separation of PEG and PLA upon particle preparation using emulsion methods (13) ensures that the particle surface is rich in biotinylated PEG, allowing facile linkage of targeting moieties, via a neutravidin bridge, to the particles at high densities. We conjugated mAbs to E-selectin, VCAM-1, or ICAM-1 to separate sets of PLA–PEG particles. As determined by FACS (Fig. 1), the level of conjugated mAb reached very high densities (in most cases $>$200,000 mAbs per particle) and was a function of the concentration of mAb used during the coupling procedure. Thus, ECAM ligands are easily coupled to the PLA–PEG particles and, by simply varying the concentration of ligand in the coupling procedure, the ligand density on the PLA–PEG particles can be controlled.

We next tested the adhesion of the mAb-conjugated PLA–PEG particles to HUVEC *in vitro*. Studies focused on understanding leukocyte adhesion to the endothelium, a process somewhat analogous to drug carrier adhesion to the endothelium, have clearly revealed that the local fluid dynamics, in particular the shear stress at the leukocyte–endothelial cell interface, can greatly influence adhesion. Indeed, adhesion events that are operative under low fluid shear conditions may not occur under physiologically relevant fluid shear conditions (30). Thus, we investigated the adhesion of the PLA–PEG particles to HUVEC under *in vitro* flow conditions that mimic fluid dynamic conditions present *in vivo*. Specifically, we used an *in vitro* flow chamber that is routinely used to study leukocyte adhesion to the endothelium under flow (26, 31).

In separate assays, we perfused the anti-E-selectin (α-E), anti-VCAM-1 (α-V), and the anti-ICAM-1 (α-I) PLA–PEG particles over inflamed HUVEC at physiologically relevant levels of fluid shear. As shown in Fig. 2, each of the leukocyte–endothelial cell adhesive particles (LEAPs) exhibited significant levels of adhesion to inflamed HUVEC. The nature of the adhesion was biphasic, wherein particles traveling at the free stream hydrodynamic velocity abruptly attached to the inflamed HUVEC and subsequently remained firmly adherent with no rolling observed. This behavior is in contrast to leukocytes that typically exhibit a rolling behavior before firm adhesion (30, 32). The adhesion of the mAb PLA–PEG particles, or LEAPs, was

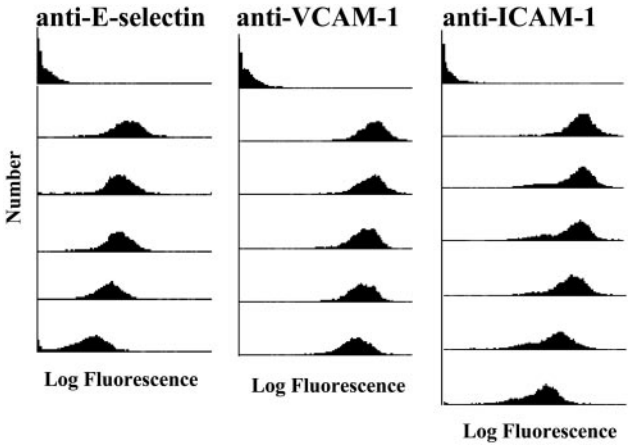

Fig. 1. mAbs to E-selectin, VCAM-1, and ICAM-1 can be coupled to PLA–PEG particles. Separate aliquots of PLA–PEG particles, precoupled with neutravidin, were incubated in solutions containing a biotinylated mAb to an ECAM at various concentrations (0, 30, 12, 6, 3, 1, or 0.5 μg/ml mAb from top to bottom, respectively). Subsequently, the particles were treated with a FITC labeled antibody and analyzed with FACS. PLA–PEG particles not treated with the FITC-labeled antibody gave results similar to the top histogram (data not shown). The 0.5 μg/ml concentration was only used for anti-ICAM-1. Results typical of $n = 5$ experiments. Calibration with Quantum Simply Cellular beads indicated that the 30 μg/ml anti-VCAM-1, anti-ICAM-1, and anti-E-selectin PLA–PEG particles had $>$200,000 bound ligands.

strikingly more avid than what was achieved previously with passive adsorption of mAbs to biodegradable particles (16). Specifically, the LEAPs exhibited significant adhesion to inflamed HUVEC at a physiologically relevant level of fluid shear (1.5 dynes/cm^2). With the previous system (16), adhesion only occurred at $\leq$0.3 dynes/cm^2, which is significantly less than physiologically relevant (i.e., $\approx$1.0 dyne/cm^2).

Neutrophils have exquisite biochemical and biophysical features that impart the ability to efficiently attach (i.e., tether) to inflamed endothelium under flow. Thus, neutrophil adhesion to inflamed HUVEC provides a standard for characterizing the level of adhesion of the LEAPs. We use our previous estimate of neutrophil primary attachment to inflamed endothelium (16) to calculate that the LEAPs achieve a level of attachment between 16% and 38% that of neutrophils. Although this represents a significant advance ($>$100-fold increase) relative to previous work (16), a more detailed comparison suggests that the LEAPs are as efficient as neutrophils at attaching to inflamed HUVEC under flow. To make the detailed comparison, it is important to realize that the primary mechanism by which particles are delivered to within molecular distance of the HUVEC monolayer in a flow chamber is the settling of the particles in response to the acceleration of gravity (33). The settling velocity scales with D^2, where D is the diameter of the particle (34). Thus, all else being equal, more neutrophils (8-μm diameter) will be delivered to within molecular distance of the HUVEC monolayer and have an opportunity to attach relative to the 2.5-μm-diameter LEAPs. Accounting for this difference in transport by using an established mathematical model (33) reveals that the efficiency of attachment of the LEAPs is equal to or perhaps greater than that of neutrophils. That is, if the same number of LEAPs and neutrophils are delivered to within molecular distance of inflamed HUVEC, the number of LEAPs that will attach to the HUVEC is equal to or exceeds the number of neutrophils that will attach. Thus, the LEAPs appear to be as efficient as neutrophils in regards to their ability to attach to inflamed HUVEC under physiologically relevant levels of fluid shear. Here, we have demonstrated biodegradable polymeric

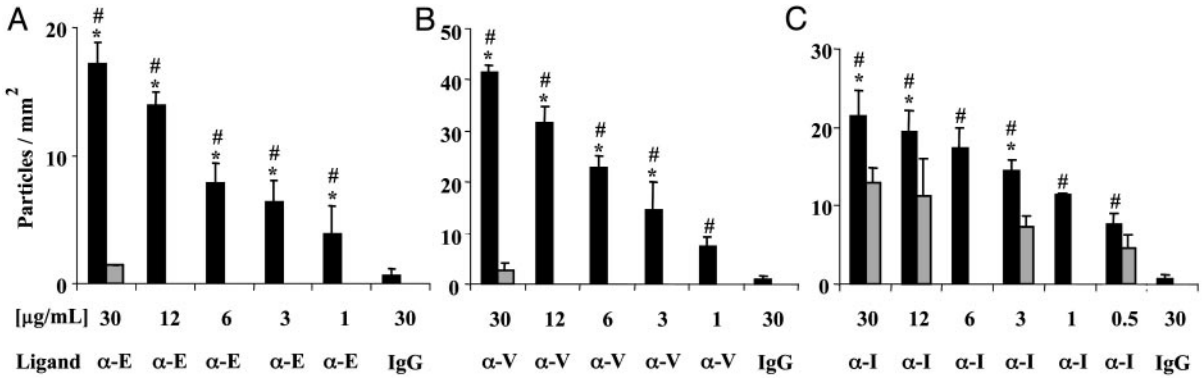

Fig. 2. LEAPs exhibit selective adhesion to cytokine activated HUVEC. Separate sets of PLA–PEG particles, conjugated with a mAb to an ECAM or mouse IgG (negative control), were perfused over HUVEC in an *in vitro* flow chamber. The number of LEAPs adherent to the HUVEC was determined after 2.5 min of flow. Black bars indicate adhesion to 4 h cytokine (IL-1β in *A* and *C* or TNF-α in *B*) activated HUVEC. Gray bars indicate adhesion to unactivated HUVEC; μg/ml is the concentration of ligand (either a mAb or mouse IgG) used during the conjugation procedure. Ligand indicates which molecule was coupled to the PLA–PEG particles, a mAb to E-selectin (α-E), VCAM-1 (α-V), ICAM-1 (α-I), or mouse IgG (IgG). Shear stress = 1.5 dynes/cm^2; $n \geq 3$; ANOVA indicated that the level of adhesion of the LEAPs to cytokine activated HUVEC was a function of the concentration of mAb used in the coupling procedure. *, $P < 0.05$ compared to LEAPs over unactivated HUVEC (gray bars); #, $P < 0.05$ compared to 30 μg/ml mouse IgG PLA–PEG particles over 4 h IL-1β or TNF-α-activated HUVEC.

particles that have adhesion efficiencies to inflamed HUVEC on par with leukocytes at physiologically relevant levels of fluid shear.

The adhesion of the LEAPs to inflamed HUVEC was significantly higher than (*i*) the adhesion of the LEAPs to noninflamed HUVEC (Fig. 2) and (*ii*) the adhesion of IgG (a negative control) PLA–PEG particles to inflamed HUVEC (Fig. 2). There are two key parameters that can be used to characterize the effectiveness of the targeting. One parameter, the selectivity, is the ratio of the number of particles delivered to the target, inflamed endothelium (for the *in vitro* model, 4-h cytokine-activated HUVEC) relative to the number of particles delivered to the noninflamed endothelium (for the *in vitro* model, HUVEC not treated with proinflammatory cytokines). The other parameter, the ligand efficiency, is the ratio of the number of targeted particles (e.g., α-E-LEAPs) delivered to the inflamed endothelium relative to the number of nontargeted particles (e.g., IgG PLA–PEG particles) delivered to the inflamed endothelium. We plotted the selectivity and ligand efficiency as a function of the concentration of mAb used in preparing the mAb PLA–PEG particles (Fig. 3).

The selectivity of LEAPs for inflamed endothelium was the greatest when VCAM-1 or E-selectin was targeted, yielding a maximal selectivity between 12 and 15 (Fig. 3*A*). Targeting ICAM-1 resulted in a rather modest selectivity of $\approx$2 (Fig. 3*A*). This modest selectivity with α-I-LEAPs reflects the fact that noninflamed HUVEC express a basal level of ICAM-1. The selectivity of α-V-LEAPs and α-E-LEAPs was a function of the concentration of mAb used in the conjugation (Fig. 3*A*). In contrast, the selectivity of α-I-LEAPs was independent of the concentration of anti-ICAM-1 used in the conjugation (Fig. 3*A*). The ligand efficiency plot (Fig. 3*B*) revealed that, for all of the LEAPs, (*i*) the addition of the mAb to the PLA–PEG particles had a dramatic effect on the adhesion to inflamed HUVEC with the ligand efficiency reaching maximal values between 27 and 33 and (*ii*) the ligand efficiency was a function of the mAb concentration used during the conjugation.

Combined, the results described above clearly demonstrate that (*i*) the efficiency of adhesion of LEAPs to inflamed HUVEC is on par with leukocytes, (*ii*) LEAPs exhibit significant selective adhesion (up to 15-fold) for inflamed HUVEC relative to noninflamed HUVEC, and (*iii*) addition of a targeting ligand significantly increases (up to 33-fold) the efficiency of adhesion of PLA–PEG particles for inflamed HUVEC. Importantly, the LEAPs exhibited this adhesive behavior under physiologically relevant fluid shear conditions.

PLA–PEG Particles Conjugated with a Recombinant PSGL-1 Construct Exhibit Significant Rolling Adhesion to Trauma-Activated Endothelium *in Vivo*. Although the *in vitro* flow chamber model captures several of the characteristics of the *in vivo* environment, it is

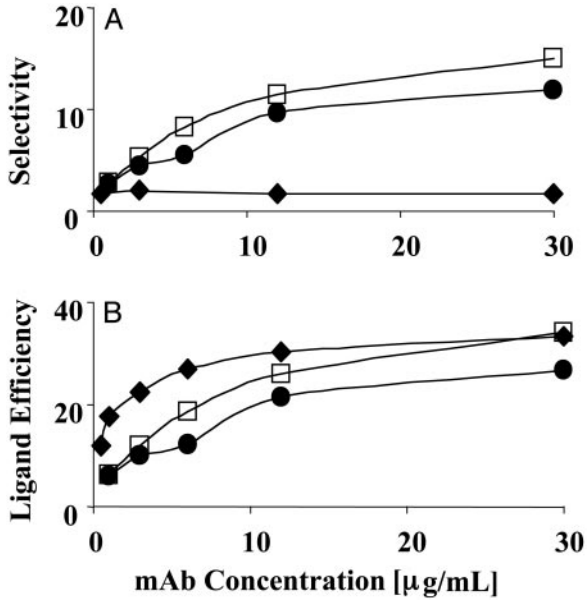

Fig. 3. The selectivity and ligand efficiency of LEAP adhesion to HUVEC. (*A*) The selectivity, defined as the ratio of the number of LEAPs that adhere to inflamed HUVEC relative to the number of LEAPs that adhere to noninflamed HUVEC, was plotted versus the concentration of mAb used in the conjugation. The selectivity is the highest for targeting VCAM-1 or E-selectin and the lowest for ICAM-1. The selectivity for VCAM-1 and E-selectin was a function of the concentration of anti-VCAM-1 and anti-E-selectin used in the conjugation, whereas the selectivity for ICAM-1 appears to be independent of concentration. (*B*) The ligand efficiency, defined as the ratio of the number of LEAPs that adhere to inflamed HUVEC relative to the number of IgG PLA–PEG particles that adhere to inflamed HUVEC, was plotted versus the concentration of mAb used in the conjugation. The ligand efficiency was a function of the concentration of mAb and reached a maximum value between 27 and 33. Open square, VCAM-1; filled circle, E-selectin; filled diamond, ICAM-1; shear stress = 1.5 dynes/cm^2.

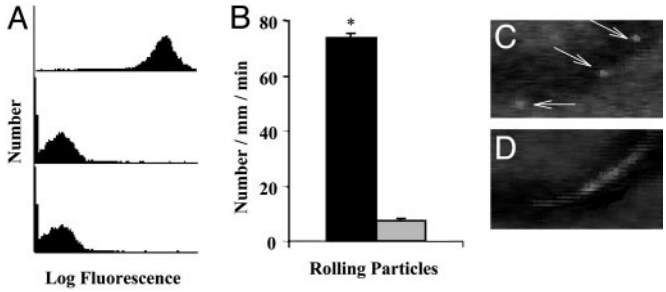

Fig. 4. PSGL-1-conjugated PLA–PEG particles adhere to trauma-activated microvascular endothelium *in vivo*. (*A*) PLA–PEG particles, precoupled with either 19.ek.Fc (a recombinant PSGL-1 construct) or ek.Fc (negative control), were treated with a mAb to human PSGL-1 (KPL-1) or human P-selectin (HPDG2/3), washed, treated with an FITC-labeled polyclonal antibody, and analyzed by FACS. (*Top*) 19.ek.Fc-LEAPs treated with a mAb to PSGL-1 (KPL-1). (*Middle*) 19.ek.Fc-LEAPs treated with a mAb to P-selectin (isotype-matched control mAb). (*Bottom*) ek.Fc PLA–PEG particles treated with a mAb to PSGL-1 (KPL-1). Results shown are typical of $n = 2$ separate experiments. (*B*) 19.ek.Fc or ek.Fc particles were injected into mice (2×10^7 per mouse), and the number of rolling particles was determined. A significantly greater number of rolling 19.ek.Fc-LEAPs was observed compared to ek.Fc PLA–PEG particles. *, $P < 0.05$. (*C* and *D*) A segment of a postcapillary venule from a typical experiment is shown. (*C*) Three images were taken 1 s apart and superimposed to generate the composite image. The white sphere (marked by the arrows) is a 19.ek.Fc-LEAP rolling along the wall of the venule. (*D*) Two images were taken 1/30th of a second apart and superimposed to generate the composite image. The white blur is a PLA–PEG particle(s) not interacting with the vessel wall.

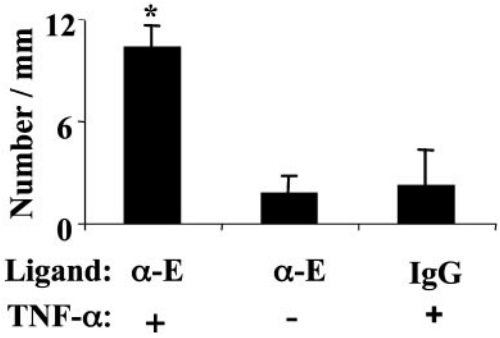

Fig. 5. α-E-LEAPs exhibit selective adhesion to TNF-α inflamed endothelium *in vivo*. Mice were given an intrascrotal injection of TNF-α or no injection. Approximately 2 h later, α-E-LEAPs or rat IgG PLA–PEG particles (negative control) were injected into the mice (5×10^6 per mouse), and the number of adherent particles was observed in the postcapillary venules of the cremaster muscle. A significantly greater number of α-E-LEAPs were adherent in TNF-α-pretreated mice compared to control mice, and a significantly greater number of α-E-LEAPs were adherent in TNF-α-pretreated mice compared to rat IgG PLA–PEG particles. All adherent particles were firmly adherent (i.e., not rolling). Ligand indicates which molecule was coupled to the PLA–PEG particles, a mAb to murine E-selectin (α-E) or rat IgG (IgG); TNF-α indicates pretreatment of mice with TNF-α 2 h before the experiment (+) or no pretreatment (−); *, $P < 0.05$ compared to right bars. FACS revealed that the α-E-mAb can be conjugated to PLA–PEG particles (data not shown).

clearly an approximation. Thus, we used intravital microscopy, a technique commonly used to study leukocyte adhesion to the endothelium *in vivo*, to determine whether the LEAPs could exhibit adhesion to inflamed endothelium *in vivo*. Exteriorizing internal tissues (e.g., cremaster muscle) is known to lead to P-selectin expression in the postcapillary vessels and subsequent leukocyte rolling that is almost exclusively mediated by P-selectin within the first hour after exteriorization of tissue (35, 36). The primary leukocyte ligand for P-selectin is PSGL-1 (22, 37). We have previously established that a recombinant PSGL-1 construct, termed 19.ek.Fc (consisting of the first 19 aa of PSGL-1 linked to an enterokinase cleavage site that is, in turn, liked to human Fc), binds to P-selectin *in vitro* and *in vivo* (21, 27, 38). The PSGL-1 portion of the 19.ek.Fc construct can be cleaved by enterokinase, leaving the Fc region (21). The enterokinase-liberated Fc (ek.Fc) serves as a negative control for the 19.ek.Fc construct (21, 27). We used these constructs and the trauma-activated model of inflammation to determine whether the LEAPs could exhibit significant adhesion *in vivo*.

FACS revealed that the 19.ek.Fc construct was coupled to the PLA–PEG particles (Fig. 4*A*). Murine cremaster muscle was exteriorized and prepared for visualization via intravital microscopy. Suspensions of 19.ek.Fc-LEAPs or ek.Fc PLA–PEG particles (negative control) were injected directly into the blood stream of groups of mice. The interaction of the particles with the postcapillary venules was observed via intravital microscopy. Approximately 10-fold more 19.ek.Fc-LEAPs exhibited an adhesive interaction with the vessel wall compared to the negative control (i.e., ek.Fc) PLA–PEG particles (Fig. 4*B*). The majority of the adhesive 19.ek.Fc-LEAPs exhibited a rolling adhesive behavior (Fig. 4*C*) that was characterized by a slow nonconstant velocity translation in the direction of flow (39). Thus, addition of the PSGL-1 peptide to the PLA–PEG particles resulted in a >10-fold increase in the adhesion of the PLA–PEG particles to the inflamed endothelium, with the majority of the adhesive 19.ek.Fc-LEAPs exhibiting a rolling adhesion. Here, we have documented targeted biodegradable polymeric particle adhesion to inflamed endothelium *in vivo* and demonstrated rolling biodegradable particles *in vivo*.

PLA–PEG Particles Conjugated with a mAb to E-Selectin Exhibit Significant Selective Firm Adhesion to TNF-α-Inflamed Endothelium *in Vivo*. It is difficult to compare LEAP adhesion to inflamed endothelium and LEAP adhesion to noninflamed endothelium by using 19.ek.Fc and the trauma model described above. To make this comparison, we investigated the adhesion of α-E-LEAPs in a TNF-α-induced model of inflammation (40). Groups of mice were given an intrascrotal injection of TNF-α, which elicits E-selectin expression (40), or no treatment. Two hours later, the cremaster muscle was prepared for observation and suspensions of α-E-LEAPs or IgG PLA–PEG particles (negative control) were injected. The number of adherent particles in the postcapillary venules was determined 10 min after the injection.

As shown in Fig. 5, 6-fold more α-E-LEAPs were adherent in TNF-α-treated mice compared to the number adherent in mice not treated with TNF-α, and 4.7-fold more α-E-LEAPs were adherent in TNF-α-treated mice compared to the number of IgG PLA–PEG particles adherent in TNF-α-treated mice. Thus, the selectivity was 6 and the ligand efficiency was 4.7. In contrast to the rolling adhesive behavior observed in the previous experiments (Fig. 4), the α-E-LEAPs exhibited a biphasic adhesive behavior, wherein particles traveling at the free-stream hydrodynamic velocity abruptly adhered and subsequently remained firmly adherent with no rolling observed. Once firmly adherent, the α-E-LEAPs remained adherent for the entire observation period (as long as 25 min). Note that the LEAPs we used in the present study are probably not endocytosed by the endothelium because of their size (41).

Combined, the data presented in Figs. 4 and 5 clearly demonstrate *in vivo* targeting to inflamed endothelium with selectivity as high as 6 and ligand efficiency as high as 10. In addition, the results demonstrate that different types of adhesion can be achieved (i.e., rolling and firm adhesion) and suggest that the nature of the adhesion can be controlled by particle design.

Conclusion

Leukocyte–endothelial cell adhesion chemistry and techniques proven indispensable for unraveling the mechanisms of leukocyte recruitment to sites of inflammation were applied to guide our design and testing of novel leukocyte-inspired biodegradable particles. This approach resulted in the generation of PEGylated biodegradable particles that exhibit highly selective accumulation on inflamed endothelium *in vitro* and *in vivo*. The LEAPs exhibit (*i*) *in vitro* attachment efficiencies to inflamed endothelium on par with that of leukocytes, (*ii*) up to 15-fold selective adhesion to inflamed endothelium under physiologically relevant *in vitro* flow conditions, (*iii*) a 6-fold selective adhesion for cytokine inflamed endothelium, relative to non-cytokine-treated endothelium, *in vivo*, and (*iv*) up to 10-fold enhancement in adhesion to trauma-induced inflamed endothelium *in vivo* due to the addition of a targeting ligand.

These results bode well for this targeting approach. However, it is important to point out other issues involved in drug delivery. For example, although the first step was to demonstrate selective adhesion to inflamed versus noninflamed endothelium and to characterize the adhesion, another key issue is to optimize selectivity for inflamed endothelium versus uptake by the reticuloendothelial system. Additionally, the possibility of unwanted effects of the particles (e.g., whether the LEAPs elicit an inflammatory response) needs to be addressed. Nevertheless, this work is clearly a significant step forward. The approach presented here and the reagents generated will foster the rational and efficient development of drug delivery schemes that seek to target drugs to diseased tissues via the heterogeneous expression of endothelial surface moieties. As the endothelium continues to be mapped, it is anticipated that opportunities for targeted drug delivery via the endothelium will further increase. A concerted and vigorous effort between investigators from a variety of disciplines, as has occurred in the field of leukocyte adhesion, will be integral to the full exploitation of these opportunities.

We thank Dr. Takahiro Morita for assistance with particle preparation and Dr. Sriram Neelamegham and Yi Zhang (Department of Chemical Engineering, State University of New York, Buffalo) for useful discussions and calculations of particle transport within the flow chamber. This work was supported by grants from The Whitaker Foundation (to D.J.G.), National Science Foundation Grants BES 9733542/0096303 (to D.J.G.) and BES0090009 (to M.F.K. and D.J.G.), the American Heart Association (M.F.K.), and a Merck Junior Faculty Development Award (to J.H.).

1. Cybulsky, M. I. & Gimbrone, M. A., Jr. (1991) *Science* **251,** 788–791.
2. Soriano, A., Salas, A., Sans, M., Gironella, M., Elena, M., Anderson, D. C., Pique, J. M. & Panes, J. (2000) *Lab. Invest.* **80,** 1541–1551.
3. Jones, S. P., Trocha, S. D., Strange, M. B., Granger, D. N., Kevil, C. G., Bullard, D. C. & Lefer, D. J. (2000) *Am. J. Physiol.* **279,** H2196–H2201.
4. Chapman, P. T., Jamar, F., Keelan, E. T., Peters, A. M. & Haskard, D. O. (1996) *Arthritis Rheum.* **39,** 1371–1375.
5. Schurmann, G. M., Bishop, A. E., Facer, P., Vecchio, M., Lee, J. C., Rampton, D. S. & Polak, J. M. (1995) *Gut* **36,** 411–418.
6. Handschel, J., Prott, F. J., Sunderkotter, C., Metze, D., Meyer, U. & Joos, U. (1999) *Int. J. Radiat. Oncol. Biol. Phys.* **45,** 475–481.
7. Prabhakarpandian, B., Goetz, D. J., Swerlick, R. A., Chen, X. & Kiani, M. F. (2001) *Microcirculation* **8,** 355–364.
8. Fox, S. B., Turner, G. D. H., Gatter, K. C. & Harris, A. L. (1995) *J. Pathol.* **177,** 369–376.
9. Spragg, D. D., Alford, D. R., Greferath, R., Larsen, C. E., Lee, K., Gurtner, G. C., Cybulsky, M. I., Tosi, P. F., Nicolau, C. & Gimbrone, M. A., Jr. (1997) *Proc. Natl. Acad. Sci.* **94,** 8795–8800.
10. Kiani, M. F., Yuan, X., Chen, L., Smith, L., Gaber, M. W. & Goetz, D. J. (2002) *Pharm. Res.* **19,** 1317–1322.
11. Everts, M., Schraa, A., de Leij, L., Meijer, D. & Molema, G. (2001) in *Drug Targeting: Organ-Specific Strategies*, eds. Molema, G. & Meijer, D. (Wiley, Weinheim, Germany), pp. 171–197.
12. Everts, M., Kok, R. J., Asgeirsdottir, S. A., Melgert, B. N., Moolenaar, T. J., Koning, G. A., van Luyn, M. J., Meijer, D. K. & Molema, G. (2002) *J. Immunol.* **168,** 883–889.
13. Gref, R., Minamitake, Y., Peracchia, M. T., Trubetskoy, V., Torchilin, V. & Langer, R. (1994) *Science* **263,** 1600–1603.
14. Soppimath, K. S., Aminabhavi, T. M., Kulkarni, A. R. & Rudzinski, W. E. (2001) *J. Control. Release* **70,** 1–20.
15. Langer, R. (1998) *Nature* **392,** 5–10.
16. Dickerson, J. B., Blackwell, J. E., Ou, J. J., Shinde Patil, V. R. & Goetz, D. J. (2001) *Biotechnol. Bioeng.* **73,** 500–509.
17. Eniola, A. O., Rodgers, S. D. & Hammer, D. A. (2002) *Biomaterials* **23,** 2167–2177.
18. Gref, R., Domb, A., Quellec, P., Blunk, T., Muller, R. H., Verbavatz, J. M. & Langer, R. (1995) *Adv. Drug Delivery Rev.* **16,** 215–233.
19. Torchilin, P. & Trubetskoy, V. S. (1995) *Adv. Drug Delivery Rev.* **16,** 141–155.
20. Dagia, N. M. & Goetz, D. J. (2003) *Am. J. Physiol.* **285,** C813–C822.
21. Goetz, D. J., Greif, D. M., Ding, H., Camphausen, R. T., Howes, S., Comess, K. M., Snapp, K. R., Kansas, G. S. & Luscinskas, F. W. (1997) *J. Cell Biol.* **137,** 509–519.
22. Sako, D., Comess, K. M., Barone, K. M., Camphausen, R. T., Cumming, D. A. & Shaw, G. D. (1995) *Cell* **83,** 323–331.
23. Bevilacqua, M. P. (1993) *Annu. Rev. Immunol.* **11,** 767–804.
24. Cannizzaro, S. M., Padera, R. F., Langer, R., Rogers, R. A., Black, F. E., Davies, M. C., Tendler, S. J. & Shakesheff, K. M. (1998) *Biotechnol. Bioeng.* **58,** 529–535.
25. Salem, A. K., Cannizzaro, S. M., Davies, M. C., Tendler, S. J., Roberts, C. J., Williams, P. M. & Shakesheff, K. M. (2001) *Biomacromolecules* **2,** 575–580.
26. Gopalan, P. K., Jones, D. A., McIntire, L. V. & Smith, C. W. (1996) in *Current Protocols in Immunology*, eds. Coligan, J. E., Kruisbeek, A. M., Margulies, D. H., Shevach, E. M. & Strober, W. (Wiley, New York), pp. 7.29.1–7.29.23.
27. Burch, E. E., Shinde Patil, V. R., Camphausen, R. T., Kiani, M. F. & Goetz, D. J. (2002) *Blood* **100,** 531–538.
28. Gimbrone, M. A., Jr., Cotran, R. S. & Folkman, J. (1974) *J. Cell Biol.* **60,** 673–684.
29. Salem, A. K., Rose, F., Oreffo, R. O. C., Yang, X. B., Davies, M. C., Mitchell, J. R., Roberts, C. J., Stolnik-Trenkic, S., Tendler, S. J. B., Williams, P. M. & Shakesheff, K. M. (2003) *Adv. Mat.* **15,** 210–213.
30. Lawrence, M. B., Smith, C. W., Eskin, S. G. & McIntire, L. V. (1990) *Blood* **75,** 227–237.
31. Goetz, D. J., Greif, D. M., Shen, J. & Luscinskas, F. W. (1998) in *Methods in Molecular Biology*, ed. Dejana, E. (Humana, Totowa, NJ), pp. 137–145.
32. Lawrence, M. B. & Springer, T. A. (1991) *Cell* **65,** 859–873.
33. Zhang, Y. & Neelamegham, S. (2002) *Biophys. J.* **83,** 1934–1952.
34. Brenner, H. (1961) *Chem. Eng. Sci.* **16,** 242–251.
35. Ley, K., Bullard, D. C., Arbones, M. L., Bosse, R., Vestweber, D., Tedder, T. F. & Beaudet, A. L. (1995) *J. Exp. Med.* **181,** 669–675.
36. Mayadas, T. N., Johnson, R. C., Rayburn, H., Hynes, R. O. & Wagner, D. D. (1993) *Cell* **74,** 541–554.
37. Moore, K. L., Patel, K. D., Bruehl, R. E., Fugang, L., Johnson, D. A., Lichenstein, H. S., Cummings, R. D., Bainton, D. F. & McEver, R. P. (1995) *J. Cell Biol.* **128,** 661–671.
38. Shinde Patil, V. R., Campbell, C. J., Yun, Y. H., Slack, S. M. & Goetz, D. J. (2001) *Biophys. J.* **80,** 1733–1743.
39. Goetz, D. J., El-Sabban, M. E., Pauli, B. U. & Hammer, D. A. (1994) *Biophys. J.* **66,** 2202–2209.
40. Kunkel, E. J. & Ley, K. (1996) *Circ. Res.* **79,** 1196–1204.
41. Wiewrodt, R., Thomas, A. P., Cipelletti, L., Christofidou-Solomidou, M., Weitz, D. A., Feinstein, S. I., Schaffer, D., Albelda, S. M., Koval, M. & Muzykantov, V. R. (2002) *Blood* **99,** 912–922.